Asian Journal of Chemistry; Vol. 37, No. 6 (2025), 1421-1430

ASIAN JOURNAL OF CHEMISTRY

https://doi.org/10.14233/ajchem.2025.33774

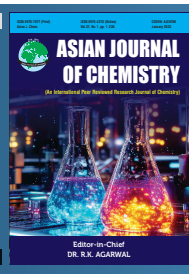

Synthesis of 1,6-Naphthyridine Derivatives and Exploration of their Corrosive Effects on 316 L Stainless Steel in Acidic Media

M.R. BHAMUNI and S.R. JAYAPRADHA*

PG and Research Department of Chemistry, Government Arts College for Women, (Affiliated to Mother Teresa Women's University, Kodaikanal), Nilakottai-624208, India

*Corresponding author: E-mail: srjayapradha2023@gmail.com

Received: 19 March 2025; *Accepted*: 13 May 2025; *Published online*: 27 May 2025; AJC-22016

Three derivatives of 1,6-naphthyridine namely (*E*)-5,7-diamino-2-(dicyanomethyl)-4-styryl-1,2,3,4-tetrahydro-1,6-naphthyridine-3,8-dicarbonitrile (**NP1**), (*E*)-5,7-diamino-4-(3-chlorostyryl)-2-(dicyanomethyl)-1,2,3,4-tetrahydro-1,6-naphthyridine-3,8-dicarbonitrile (**NP2**) and (*E*)-5,7-diamino-4-(3-bromostyryl)-2-(dicyanomethyl)-1,2,3,4-tetrahydro-1,6-naphthyridine-3,8-dicarbonitrile (**NP3**) were synthesized through a one pot cascade reaction of aromatic aldehydes and malononitrile dimer in the presence of ethanol as a solvent under reflux mode for 4-6 h and characterized by ^{1}H, ^{13}C NMR, FT-IR and UV-Vis spectroscopies. Since naphthyridine derivatives possess a wide range of biological activities and the synthesized naphthyridine derivatives then subjected to antimicrobial activities. Furthermore, studies on the corrosion inhibition activity of novel naphthyridine derivatives (**NP1**, **NP2** and **NP3**) was performed in 20% HCl on 316 L stainless steel and show very good corrosion inhibition activity. The corrosion study was carried out *via* electrochemical impedance spectroscopy (EIS), potentiodynamic polarization (PDP), weight loss method and scanning electron microscopy (SEM). The results show that derivative **NP2** has a maximum inhibition efficiency of 83.7% at 40 ppm. The potentiodynamic polarization curves demonstrated that all the three naphthyridine derivatives (**NP1**, **NP2** and **NP3**) act as mixed-type. SEM revealed that all the three naphthyridine inhibitors were adsorbed on the surface of 316 L SS and acted as a protective layer.

Keywords: Naphthyridine, Aldehyde, Malononitrile dimer, Biological activities, 316 L stainless steel, Corrosion inhibitor.

INTRODUCTION

Naphthyridines are a class of heterocyclic compounds also called "benzodiazines" or "diazanaphthalenes", they possess a fused system of two pyridine rings. There are six positional isomers with different locations of nitrogen atoms [1]. Naphthyridines have many biological applications such as anti-asthmatic, antibacterial and antimalarial agents, antimicrobial, antitumor, anti-inflammatory, anti-osteroporotic, anti-allergic, gastric antisecretory, bronchodilators activities *etc.*, [2]. Among the different naphthyridine derivatives 1,6-naphthyridine unit has been synthesized in a simple and non-conventional way and it has a wide range of biological activities such as in medicinal chemistry and mainly focused on cancer treatment [3]. Naphthyridine compound has six different isomeric forms such as 1,5-naphthyridine, 1,6-naphthyridine, 1,7-naphthyridine, 1,8-naphthyridine, 2,6-naphthyridine and 2,7-napthyridine. These derivatives are particularly useful in therapeutic areas and in the field of medicinal chemistry and pharmaceutical properties [4].

Malononitrile derivatives serve as crucial components in the synthesis of both carbo and heterocyclic compounds. They act as reagents for the preparation of synthetic dyes and various heterocyclic derivative compounds, significantly contributing to the formation of a crystalline compound known as malononitrile dimer (2-aminopropene-1,1,3-tricarbonitrile or 2-amino-1,1,3-tricyanopropene) [5]. The methylene group in malononitrile dimer can be easily reacted with carbonyl or nitroso compounds to produce various magenta and yellow-coloured dyes. It is possible to obtain bright cyan dyes from bisacylation of amino group in magenta dyes containing malononitrile dimer as an acceptor [6]. The push-pull chromophores are a group of organic compounds used in various fields, the malononitrile type of chromophores are developed in recent days [7]. The malononitrile

dimer synthesizes the hydroxytricyanopyrrole (HTCP) acceptor when interacting with diacetyl by a catalytic amount of sodium hydroxide. Furthermore, it can react with aldehyde to prepare vinylene-HTCP and a novel group of chromophores was obtained [8]. This dimer has a variety of applications especially in medicinal and pharmaceutical industries, to improve nerve growth factors [9]. It decreases the risk factor of amnesia induced by electroconvulsive shock and also exists as nootropic activity.

Malononitrile dimer is an electron acceptor group because of three CN functional group; this advantage makes the reaction flexible and high reactivity to produce the targeted compound [10,11]. A wide range of key materials to synthesize 1,6-naphthyridine derivatives by cyclization reaction. The cyclization happens in both inter and intramolecular regions to obtain naphthyridine derivatives. The simple hydrogenolysis of 4-chloro-1,6-naphthyridine to form 1,6-naphthyridine derivatives by two-step process of using hydrazine and then oxidation with copper sulphate in the presence of kieselguhr [12]. The many other possible ways to synthesize naphthyridine derivatives from nicotinic acid, nicotinaldehyde, nicotinamides, pyridine-3-carbonitrile, 1-isocyanato-2-benzene, 3-halopyridine, pyridine-6-carbaldehyde, quinoline, isoquinoline, piperidinones, aryl acrylic acid, azaisatoic anhydride, methyl ketones, benzaldehyde and propanenitrile derivatives [13]. In addition to the above literature survey reveals that the naphthyridine derivatives are used as a strong corrosion inhibitor since it has higher efficiency [14-20]. This work describes the synthetic potential of malononitrile dimer as a convenient precursor and multifunctional reagent for assembling 1,6-naphthyridine derivatives (**NP1**, **NP2** and **NP3**). It was confirmed by spectral analysis of ^{1}H, ^{13}C NMR, FT-IR, UV visible and also evaluated for the antimicrobial studies against Gram-positive and Gram-negative bacteria. Furthermore, the synthesized the naphthyridine derivatives were also studied their corrosion inhibition behaviour on 316L stainless steel in 20% HCl using electrochemical impedance spectroscopy, potentiodynamic polarization measurement, weight loss method and scanning electron microscopy. spectrometer. The UV-Vis absorption spectra were recorded on a Perkin-Elmer UV-360 instrument at wavelength ranging from 800-200 nm. The SEM analysis was performed to study the surface of 316 L SS surface without and with inhibitors (**NP1**, **NP2** and **NP3**) after 5 h immersion at room temperature *via* a VEGA 3 TESCAN instrument (USA).

EXPERIMENTAL

Commercially available compounds such as triethanolamine, ethanol and triethanolamine were bought from Sigma-Aldrich and used without any further purification. The reaction was monitored by TLC using Merck TLC silica gel 60 F_{254} plates. A Bruker 400 MHz instrument was used to record ^{1}H NMR spectra with $CDCl_3$ as solvent and TMS as internal standard. The same instrument was used to record the ^{13}C NMR at 125 MHz. The FT-IR spectra were recorded in the range of 4000 400 cm^{-1} by an FTIR-PRO-ONE spectrometer. The UV-Vis absorption spectra were recorded on a Perkin-Elmer UV-360 instrument at wavelength ranging from 800-200 nm. The SEM analysis was performed to study the surface of 316 L SS surface without and with inhibitors **NP1**, **NP2** and **NP3** after 5 h immersion at room temperature using a VEGA 3 TESCAN instrument (USA).

Preparation of malononitrile dimer: Sodium hydroxide (8 g, 0.2 mL) dissolved in 50 mL of water and 50 g of cupric sulfate pentahydrate dissolved in 100 mL of warm water were added 13.2 mL (0.2 mL) of malononitrile. The insoluble inorganic salt was removed by heating the mixture at 90 ºC. The mixture subsequently cooled and the crude crystals of the formed malononitrile dimer (4.5 g) was recrystallized from water [21].

Inhibitor synthesis

(*E*)-5,7-Diamino-2-(dicyanomethyl)-4-styryl-1,2,3,4-tetrahydro-1,6-naphthyridine-3,8-dicarbonitrile (NP1): A mixture containing cinnamaldehyde (0.01 M, 1.32 g), malononitrile dimer (0.02 M, 2.64 g), triethanolamine (0.01 M, 1.49 g) and ethanol (15 mL) was refluxed for 4-6 h. On cooling the mixture at room temperature, the solid precipitate was filtered out (**Scheme-I**). ^{1}H NMR (400 MHz, $CDCl_3$) δ ppm: 2.49-2.71 (3H, 2.56 (dtd, *J* = 4.6, 3.7, 1.9 Hz), 2.66 (d, *J* = 3.7 Hz), 3.59 (1H, dd, *J* = 5.0, 4.6 Hz), 4.24-4.46 (2H, 4.30 (dd, *J* = 6.4, 1.9 Hz), 4.41 (d, *J* = 6.4 Hz)), 6.38-6.58 (2H, 6.46 (d, *J* = 16.9 Hz), 6.50 (dd, *J* = 16.9, 5.0 Hz)), 7.19 (1H, tt, *J* = 7.7, 1.3 Hz), 7.25-7.48 (4H, 7.32 (dddd, *J* = 7.7, 7.6, 1.8, 0.5 Hz), 7.42 (dddd, *J* = 7.6, 1.8); ^{13}C NMR (125 MHz, $CDCl_3$) δ ppm: 37.5 (1C, s), 42.6 (1C, s), 48.1 (1C, s), 51.8 (1C, s), 67.0 (1C,

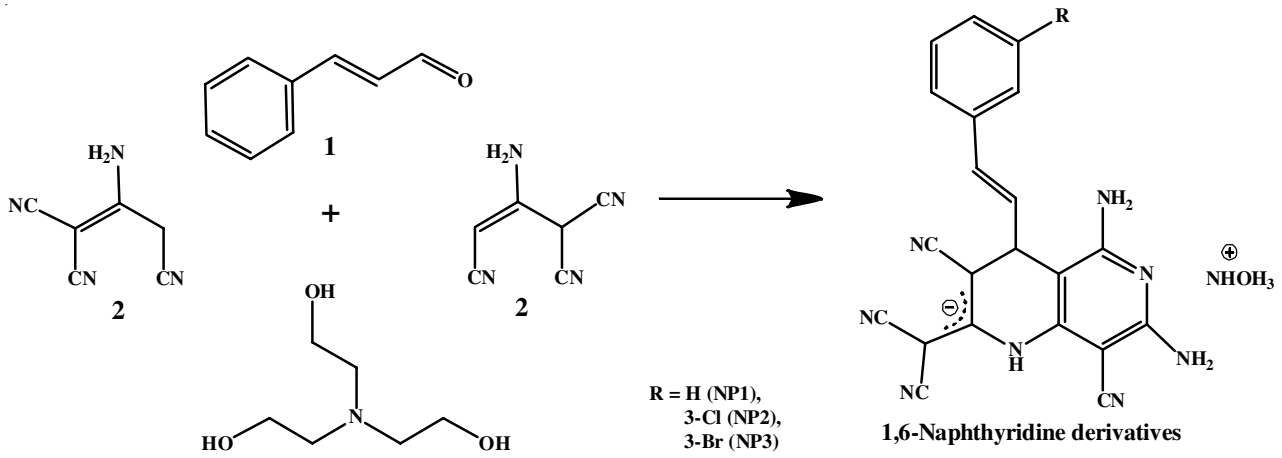

Scheme-I: Synthesis of 1,6-naphthyridine derivatives (**NP1-NP3**)

s), 112.0 (1C, s), 112.4 (1C, s), 112.9-113.0 (2C, 112.9 (s), 112.9 (s)), 115.2 (1C, s), 127.3 (2C, s), 128.1 (1C, s), 128.6 (2C, s), 133.4 (1C, s), 133.8 (1C, s), 134.8 (1C, s), 138.5 (1C, s), 157.7 (1C, s), 160.1 (1C, s).

(*E*)-5,7-Diamino-4-(3-chlorostyryl)-2-(dicyanomethyl)-1,2,3,4-tetrahydro-1,6-naphthyridine-3,8-dicarbonitrile (NP2): A mixture containing 3-chlorocinnamaldehyde (0.01 M, 1.66 g), malononitrile dimer (0.02 M, 2.64 g), triethanolamine (0.01 M, 1.49 g) and ethanol (15 mL) was refluxed for 4-6 h. On cooling the mixture at room temperature, the solid precipitate was filtered out. ^{1}H NMR (400 MHz, $CDCl_3$) δ ppm: 3.76-3.93 (2H, 3.82 (dd, *J* = 4.6, 1.9 Hz), 3.87 (dd, *J* = 4.9, 4.6 Hz), 4.41 (1H, d, *J* = 6.3 Hz), 4.71 (1H, dd, *J* = 6.3, 1.9 Hz), 6.42-6.65 (2H, 6.50 (dd, *J* = 16.9, 4.9 Hz), 6.58 (d, *J* = 16.9 Hz)), 7.18-7.55 (4H, 7.25 (ddd, *J* = 8.1, 1.7, 1.4 Hz), 7.37 (ddd, *J* = 8.1, 8.0, 0.6 Hz), 7.41 (ddd, *J* = 8.0, 1.7, 1.4 Hz), 7.49 (td, *J* = 1.7, 0.6 Hz); ^{13}C NMR (125 MHz, $CDCl_3$) δ ppm: 37.5 (1C, s), 50.8 (1C, s), 51.8 (1C, s), 67.0 (1C, s), 112.0 (1C, s), 112.4 (1C, s), 112.9-113.0 (2C, 112.9 (s), 112.9 (s), 115.2 (1C, s), 117.7 (1C, s), 127.0 (1C, s), 127.3 (1C, s), 127.7 (1C, s), 129.2 (1C, s), 129.4 (1C, s), 133.1 (1C, s), 133.4 (1C, s), 133.8 (1C, s), 138.5 (1C, s), 157.7 (1C, s), 160.1 (1C, s).

(*E*)-5,7-Diamino-4-(3-bromostyryl)-2-(dicyanomethyl)-1,2,3,4-tetrahydro-1,6-naphthyridine-3,8-dicarbonitrile (NP3): A mixture containing 3-bromocinnamaldehyde (0.01 M, 2.11 g), malononitrile dimer (0.02 M, 2.64 g), triethanolamine (0.01 M, 1.49 g) and ethanol (15 mL) was refluxed for 4-6 h. On cooling the mixture at room temperature, the solid precipitate was filtered out. ^{1}H NMR (400 MHz, $CDCl_3$) δ ppm: 3.76-3.93 (2H, 3.82 (dd, *J* = 4.6, 1.9 Hz), 3.87 (dd, *J* = 4.9, 4.6 Hz)), 4.41 (1H, d, *J* = 6.3 Hz), 4.71 (1H, dd, *J* = 6.3, 1.9 Hz), 6.42-6.57 (2H, 6.50 (dd, *J* = 16.9, 4.9 Hz), 6.49 (d, *J* = 16.9 Hz)), 7.23-7.48 (4H, 7.29 (dt, *J* = 8.1, 1.8 Hz), 7.33 (dt, *J* = 8.0, 1.8 Hz), 7.35 (ddd, *J* = 8.1, 8.0, 0.6 Hz), 7.42 (ddd, *J* = 1.9, 1.8, 0.6 Hz). ^{13}C NMR (125 MHz, $CDCl_3$) δ ppm: 37.5 (1C, s), 50.8 (1C, s), 51.8 (1C, s), 67.0 (1C, s), 112.0 (1C, s), 112.4 (1C, s), 112.9-113.0 (2C, 112.9 (s), 112.9 (s), 115.2 (1C, s), 117.7 (1C, s), 121.2 (1C, s), 127.3 (1C, s), 129.2 (1C, s), 129.4 (1C, s), 129.7 (1C, s), 130.6 (1C, s), 133.4 (1C, s), 133.8 (1C, s), 138.5 (1C, s), 157.7 (1C, s), 160.1 (1C, s).

Electrochemical measurements: The electrochemical measurements were performed in a three-electrode-cell. The 316L stainless steel (SS) sample was subjected to a cleaning process, which involved washing with acetone, followed by drying at room temperature and used as a working electrode, with platinum as the counter electrode and the saturated calomel electrode as the reference electrode.

Electrochemical impedance spectroscopy (EIS): The EIS measurement for the synthesized compounds **NP1**, **NP2** and **NP3** were calculated by Nyquist plot, the inhibition efficiency (IE%) of the naphthyridine inhibitors using the following equation [22]:

$$IE\ (\%) = \frac{(R_{ct} - R_{ct}^{o})}{R_{ct}} \times 100 \quad (1)$$

where R_{ct} = charge transfer resistance with inhibitors; R_{ct}^{o} = charge transfer resistance without inhibitors.

The surface morphology (316 L SS) coverage (θ) was calculated using eqn. 2:

$$\theta = \frac{(C_{dl}^{o} - C_{dl})}{C_{dl}^{o}} \quad (2)$$

where C_{dl}^{o} and C_{dl} are the double-layer capacitance values without and with **NP1**, **NP2** and **NP3** inhibitors.

Potentiodynamic polarization measurement (PDP): The potentiodynamic polarization measurements for the corrosion inhibitors **NP1**, **NP2** and **NP3** were designed from the Tafel plots and the inhibition efficiency (IE %) of the inhibitors was calculated using eqn. 3 [23]:

$$IE\ (\%) = \frac{I_{corr} - I_{corr\,(inhibitor)}}{I_{corr}} \times 100 \quad (3)$$

where, I_{corr} and $I_{corr\ (inhibitor)}$ are the values of current densities without and with inhibitors **NP1**, **NP2** and **NP3**.

Weight loss measurements: A weight loss measurement is an immersion test to identify the metal performance using inhibitors **NP1**, **NP2** and **NP3**. The corrosion presentation of 316 L SS in 20% HCl solutions without and with inhibitors was investigated by the weight loss measurements by the side of the immersion times investigated were 168, 336, 504 and 672 h. From the weight loss outcome, the corrosion rate (W) values were calculated by the following expression [24]:

$$W = \frac{m_1 - m_2}{S \times t} \quad (4)$$

where m_1 and m_2 are the weight losses of without and with inhibitors, S is the surface area of the sample (cm^2), t is the immersion time (h).

By using the corrosion rate (W) values, the inhibition efficiency IE (%) was calculated using eqn. 5:

$$IE\ (\%) = \frac{W_{blank} - W_{inh}}{W_{blank}} \times 100 \quad (5)$$

where W_{blank} and W_{inh} are the corrosion rates of 316 L SS without and with the inhibitor.

RESULTS AND DISCUSSION

To synthesize (*E*)-5,7-diamino-2-(dicyanomethyl)-4-styryl-1,2,3,4-tetrahydro-1,6-naphthyridine-3,8-dicarbonitrile (**NP1**), first prepared malononitrile dimer (**2**) from malononitrile, NaOH and cupric sulfate pentahydrate. Reflux between substituted cinnamaldehyde *e.g.* Cl (**NP2**), Br (**NP3**) and malononitrile dimer (**2**) in triethanolamine using ethanol as solvent has afforded as a product [25] in high yields. This work aims to synthesize highly efficient compounds of azaheterocycles by a cascade reaction, because the iminium anion reacts with a nucleophilic reagent and then reacts with the electrophilic center to form pyrrole or pyridine heterocyclic compounds. The malononitrile dimer (**2**) has three cyano groups and can easily form an azaheterocyclic compound by a cascade reaction. The cascade reaction is also known as a tandem or domino reaction that comprises two consecutive reactions. The cascade transformation in this review from intermediate **A** to form a compound **D** and then to the complex product **(NP1)** by the stepwise process in

Scheme-II. We reported that azaheterocycles formed by one pot synthesis under reflux for 6 h in the presence of ethanol as a solvent at room temperature from malononitrile dimer (**2**) and aldehyde (**1**) and that the reactions were carried out by microwave irradiation with aldehydes and malononitrile dimer. It is difficult to perform this process in the presence of other solvents such as toluene, benzene and acetone because dimer easily dissolves in alcohol.

The proposed mechanism in **Scheme-II** can explain the structure of derivative **NP1**. Under reaction conditions, mixture of cinnamaldehyde (**1**), malononitrile dimer (**2**) and drops of TEOA form a Michael adduct **A**, amino group are added to the imine group by electrophilic carbon atoms and intermediate **B** is formed. The diazabicyclic compound of **C** occurred due to the close proximity of the amino and cyano groups. Finally the formation of compound **D** by ring opening leads to the formation of (*E*)-5,7-diamino-2-(dicyanomethyl)-4-styryl-1,2,3,4-tetrahydro-1,6-naphthyridine-3,8-dicarbonitrile (**NP1**) in excellent yield. The quantum chemical studies for intermediate **A** show that cyclization only happens when the participation of dicyanomethylene fragments gets targeted results.

Thus, the above protocol clarified the structure of the product (*E*)-5,7-diamino-2-(dicyanomethyl)-4-styryl-1,2,3,4-tetrahydro-1,6-naphthyridine-3,8-dicarbonitrile **(NP1)** with cinnamaldehyde (**1**), malononitrile dimer (**2**) and triethanolamine. Column chromatography is not necessary to purify the

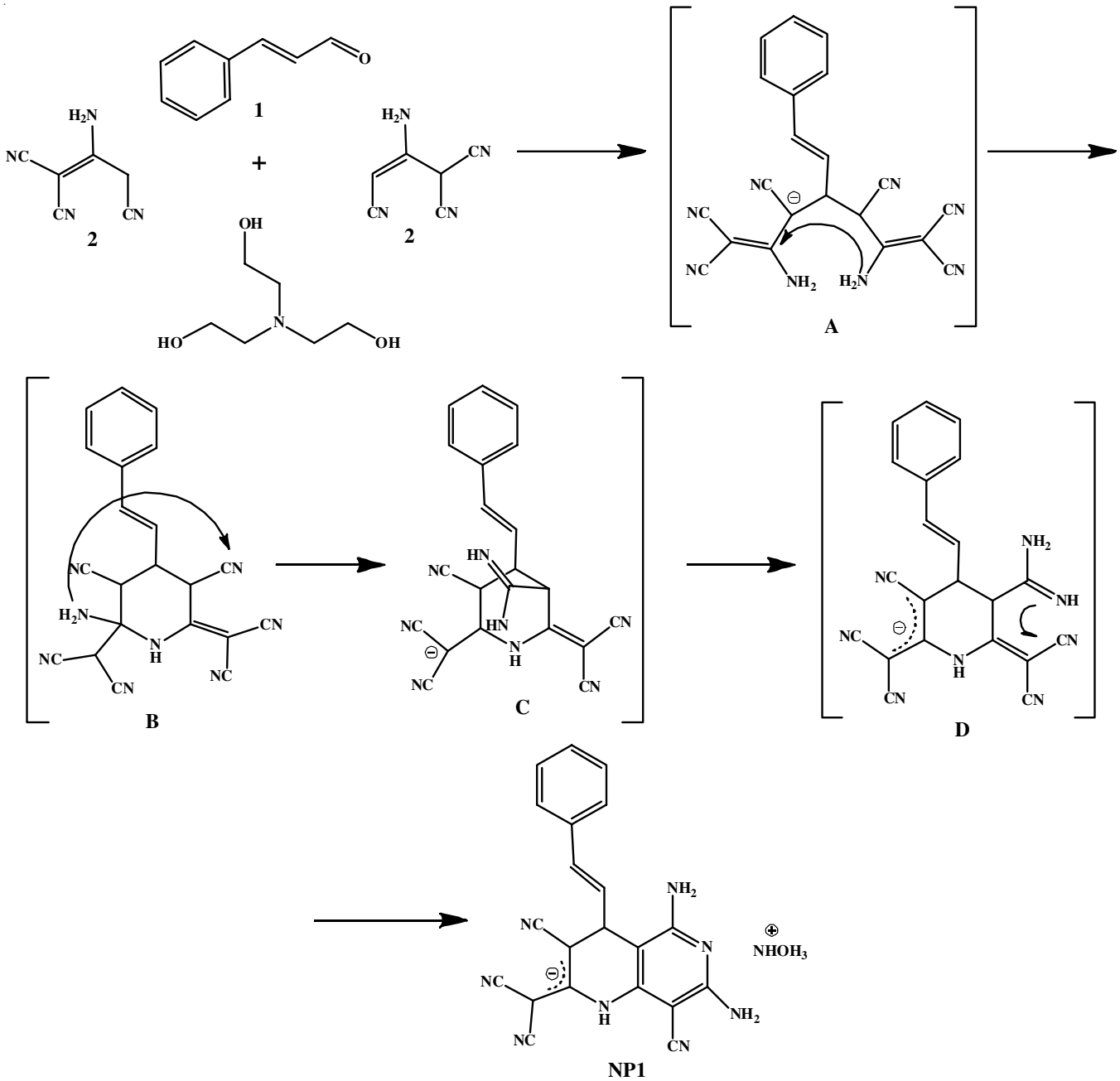

Scheme-II: Mechanism for the synthesis of (*E*)-5,7-diamino-2-(dicyanomethyl)-4-styryl-1,2,3,4-tetrahydro-1,6-naphthyridine-3,8-dicarbonitrile (**NP1**)

products; the structure of the synthesized compound (**NP1**) was confirmed by spectral studies such as FT-IR, UV visible, ^{1}H and ^{13}C NMR. The compound (**NP1**) was also evaluated for biological studies.

FT-IR and UV-vis spectral studies: The FT-IR spectra of the synthesized naphthyridine derivatives **NP1**, **NP2** and **NP3** were characterized in the absorption bands of the hydroxyl group and the NH- fragments appeared at ~3253 cm^{-1} (**NP1**), ~3291 cm^{-1} (**NP2**) and ~3294 cm^{-1} (**NP3**). The strong intense bands at ~2201 cm^{-1} (**NP1**), ~2212 cm^{-1} (**NP2**) and ~2220 cm^{-1} (**NP3**) are attributed to conjugated cyano groups. The peaks at ~3072 cm^{-1}, ~719 cm^{-1} (**NP1**), ~794 cm^{-1} (**NP2**) and ~790 cm^{-1} (**NP3**) are C-H stretching frequency. The C=C bonds at ~1593 cm^{-1} and the aromatic region is located at ~1438 cm^{-1} (**NP2**1, **NP2** & **NP3**). Moreover, the chloro and bromo groups appear at ~743 cm^{-1} (**NP2**) and ~650 cm^{-1} (**NP3**), respectively. All the FT-IR results showed that compounds **NP1**, **NP2** and **NP3** formed well (Table-1). The UV-vis absorption for naphthyridine derivatives **NP1**, **NP2** and **NP3** shows absorbance band from 200 to 600 nm, the strong adsorption bands at 344 nm (**NP1**), 239 (**NP2**) and 229 (**NP3**) suggested that the π-π* and n-π* transition. It is very well known that the naphthyridine derivatives obtained well.

^{1}H and ^{13}C NMR spectra: The ^{1}H NMR spectrum of compound **NP1** shows broad signals of hydroxyl protons at δ 7.33-7.16 ppm. The compound **NP1** showed two singlets at δ = 6.51 ppm and δ = 6.43 ppm each for one proton of the naphthyridine ring. The significant signals of singlets appeared in the region of δ 4.73 ppm, 4.32 ppm and 3.40 ppm. The ^{13}C NMR spectrum for compound **NP1** has signals at C-atoms of the second and fourth positions of two pyridine rings, which are the naphthyridine rings at δ 161.75 and 158.33 ppm. The signals of C-atoms in the fifth and third position are due to 91.50 ppm. The ^{13}C NMR signals of the cyano group appear at the signals of δ 114.60-114.21 ppm and 114.02 ppm. The other fragments of C-atoms at δ 67.88, 55.75, 47.18, 34.59 and 23.43 ppm, respectively. Then the doublet of doublet patterns at δ 3.93 ppm, 3.87 ppm, 4.71 ppm and 6.65 ppm. This confirms compound **NP2** for proton NMR formation and carbon NMR shows the singlet at δ 37.5, 50.8, 51.8, 67.0, 112.0, 113.0, 115.2, 117.7, 127.0, 127.3, 129.2, 133.4, 138.5 confirms the presence of pyridine ring in naphthyridine derivatives. For compound **NP3** has the peaks at δ 3.82 ppm, 3.87 ppm, 6.50 ppm, the doublet of doublet pattern indicates the naphthyridine formation and ^{13}C NMR signals appears at δ 37.5, 50.8, 51.8, 67.0, 112.0, 112.4, 113.0, 112.9, 115.2, 117.7, 121.2, 127.3 for pyridine position in naphthyridine compound.

Antimicrobial studies: The biological activities of the 1,6-naphthyridine derivatives, which has active antimicrobial potential were also explored. The antimicrobial activity of the synthesized compounds **NP1**, **NP2** and **NP3** against various bacterial strains was evaluated by diffusion method. Amikacin was used as a standard disc for testing bacterial cultures by Kirby-Bauer method. This method is also known as the disc-diffusion antibiotic susceptibility test, the diffusion antibiotic sensitivity test and the agar diffusion test. The agar plates were incubated overnight to measure the presence or absence of zones of incubation in the disks. The antibiotic kills the bacteria or stops growth, indicating that the area around the disks is known as the zone of inhibition. After a particular number of hours of incubation, the zone of incubation was measured with a metric ruler and the diameter of the disc was measured. The bacteria grown on the agar plate were used as positive controls because growth inhibition occurred on the plates [26].

The synthesized compounds **NP1**, **NP2** and **NP3** showed significant antibacterial activity against Gram-positive and Gram-negative bacterial strains. For antimicrobial studies, incubation was carried out at 35 ºC for 48 h. The compounds were tested at a concentration of 100 µL (dilution) in acetone against all the organisms. The zone of inhibition was calculated in millimeters and compared with that of the standard disc. The significant inhibition of naphthyridine compounds was due to the CN and NH groups present on the benzene ring (Table-2).

TABLE-1
FT-IR SPECTRAL PEAK OF THREE NAPHTHYRIDINE DERIVATIVES

NP1		**NP2**		**NP3**	
Bands	Band assignment	Bands	Band assignment	Bands	Band assignment
3253	N-H stretching	3291	N-H stretching	3294	N-H stretching
3072	C-H stretching	2212	C≡N stretching	2220	C≡N stretching
2201	C≡N stretching	1618	C=C stretching	1662	C=C stretching
1593	C=C stretching	1438	Aromatic ring stretching	1438	Aromatic ring stretching
1438	Aromatic ring stretching	794	C-H stretching	790	C-H stretching
719	C-H stretching	743	C-Cl stretching	650	C-Br stretching

TABLE-2
ANTIMICROBIAL ACTIVITY RESULTS OF **NP1**, **NP2** AND **NP3**

Gram-positive bacteria				Gram-negative bacteria			
Organisms	**NP1**	**NP2**	**NP3**	Organisms	**NP1**	**NP2**	**NP3**
Staphylococcus aureus	16 mm	14 mm	17 mm	*Escherichia coli*	14 mm	20 mm	22 mm
Staphylococcus epidermidis	26 mm	16 mm	20 mm	*Klebsiella oxytoca*	22 mm	12 mm	15 mm
Bacillus subtilis	14 mm	12 mm	18 mm	*Salmonella typhi*	20 mm	15 mm	18 mm
Salmonella typhimurium	15 mm	18 mm	22 mm	*Shigella dysentery*	22 mm	19 mm	24 mm
Bacillus cereus	14 mm	22 mm	15 mm	*Vibrio cholerae*	18 mm	20 mm	16 mm

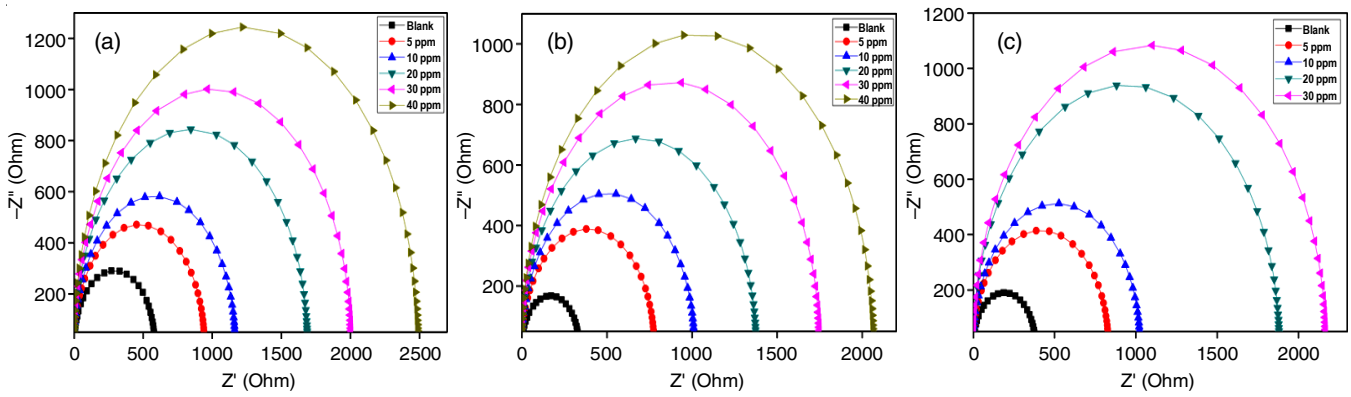

Fig. 1. Nyquist plots of 316 L SS in 20% HCl solution in absence and the presence of naphthyridine inhibitors (a) **NP1** (b) **NP2** (c) **NP3** at various concentrations

Characterization of corrosion inhibition and its evaluation

Electrochemical impedance spectroscopy (EIS): The EIS of the corrosion inhibitors **NP1**, **NP2** and **NP3** on 316 L SS dipped in 20% HCl solution for 30 min. Fig. 1 represents the Nyquist plot in absence and presence of inhibitors acid solution contains different concentrations (5 ppm, 10 ppm, 20 ppm, 30 ppm, 40 ppm, 50 ppm, 70 ppm and 100 ppm) the corrosion performance on metal surface depends on the character of the functional group present in inhibitors **NP1**, **NP2** and **NP3**. The semicircle in the Nyquist plot shows the corrosion inhibitors increased continuously with increasing concentration. Fig. 1a-b shows the equivalent circuit in absence and presence of inhibitors, determined with the help of Zsimpwin software and the values are summarized in Table-3. Fig. 2a circuit represents the absence of inhibitor and Fig. 2b indicates the circuit for presence of inhibitors **NP1**, **NP2** and **NP3**, it exist R_s meant for solution resistance, the R_{ct} indicates the charge transfer resistance and the C_{dl} represents the double layer capacitance and the L is inductor existing an exact fit.

Fig. 1a indicates the Nyquist plot on 316 L SS in 20% HCl solution in absence and the presence of **NP1** inhibitor and the EIS data of **NP1** inhibitor. From EIS studies of **NP1** inhibitor, as the amount of **NP1** inhibitor increased, the resistance to charge transfer increased, while the capacitance of the double layer decreased (Table-3). There is no change obtained after the concentration of 40 ppm, this may be due to the functional

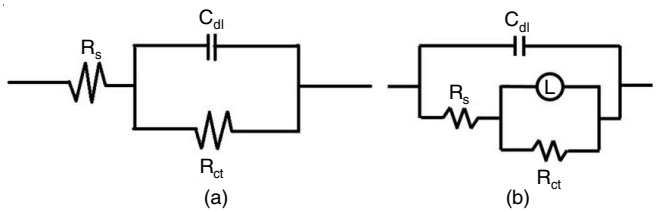

Fig. 2. The circuit used to fit for the corrosive solution of (a) blank-20% HCl solution (b) presence of the inhibitors (**NP1**, **NP2** and **NP3**)

groups in **NP1** inhibitor such as N-H, C≡N, C=C, C-H groups are strongly absorbs the metal surface on 316 L stainless steel to form a protective layer. The EIS results suggested that **NP1** inhibitor act as a moderate corrosion inhibitor, which showed the greatest inhibition efficiency 76.4% at 40 ppm concentration, after 40 ppm the inhibition efficiency gradually decreases. Likewise, Fig. 1b shows nyquist plot figure of 316L SS in 20% HCl solution in absence and the presence of **NP2** inhibitor. The EIS data of **NP2** inhibitor in Table-3 shows that the R_{ct} values increases and the C_{dl} values decrease with increasing the **NP2** inhibitor concentration up to 40 ppm, furthermore there is no change occurred after 40 ppm because the protective film formed on 316 L SS surface and showed the maximum inhibition efficiency of 83.7% at 40 ppm concentration. The EIS results of **NP2** inhibitor acts as a good corrosion inhibitor on stainless steel metal surface. Fig. 1c indicates the Nyquist plot of 316 L SS in 20% HCl solution in the absence and

TABLE-3
EIS RECORDS OF 316L SS IN 20% HCl SOLUTION FOR THREE INHIBITORS
(**NP1**, **NP2** AND **NP3**) AT DIFFERENT CONCENTRATIONS

Inhibitor conc. (ppm)	NP1				NP2				NP3			
	R_{ct} (Ω cm^2)	C_{dl} (10^{-5} F cm^2)	Surface coverage (θ)	IE (R%)	R_{ct} (Ω cm^2)	C_{dl} (10^{-5} F cm^2)	Surface coverage (θ)	IE (R%)	R_{ct} (Ω cm^2)	C_{dl} (10^{-5} F cm^2)	Surface coverage (θ)	IE (R%)
Blank	588	810	–	–	337	1132	–	–	383	299.8	–	–
5	943	505	0.37	37.6	778	490	0.65	65.9	827	358	0.53	53.6
10	1166	408	0.49	49.5	1014	376	0.68	68.5	1024	285	0.62	62.5
20	1696	280	0.65	65.3	1376	277	0.73	73.1	1883	155	0.79	79.6
30	2007	241	0.70	70.7	1747	218	0.76	76.1	2165	134	0.82	82.3
40	2494	192	0.76	76.4	2071	184	0.82	82	1792	163	0.78	78.6
50	1756	275	0.66	66.5	1672	228	0.81	81.2	1259	232	0.69	69.5
70	1232	387	0.52	52.2	1291	296	0.71	71.1	907	322	0.57	57.7
100	1066	448	0.44	44.8	964	396	0.69	69.1	823	355	0.53	53.4

presence of **NP3** inhibitor. From Fig. 1c, impedance behaviour of 316L SS has increasing concentration of **NP3** inhibitor. The EIS records of the **NP3** inhibitor in Table-3 explains the R_{ct} values increase and the C_{dl} decrease with increasing the **NP3** inhibitor concentration up to 30 ppm and a more increase in concentration of **NP3** do not show in the least significant change. This suggested that the **NP3** inhibitor completely occupy the metal surface of 316 L SS. The EIS results of **NP3** inhibitor act as a very good inhibitor and the maximum inhibition efficiency of 78.6% at 30 ppm concentration. The EIS results of three inhibitors **NP1**, **NP2** and **NP3** showed the inhibition efficiencies of 76.4% at 40 ppm, 83.7% at 40 ppm and 78.6% at 30 ppm for **NP1**, **NP2** and **NP3** inhibitors, respectively. Among all the studies of EIS corrosion inhibitors, the **NP2** has the highest inhibition efficiency 88% at 50 ppm. This may be due to the effect of more functional groups namely N-H, C≡N, C=C, C-H, Br and Cl are present in the **NP2** when compared with the other two inhibitors. This suggests that **NP2** corrosion inhibitor is robustly adsorbed on surface coverage of 316L SS. Then order of the three inhibitors follows the inhibition efficiency of **NP2** > **NP3** > **NP1**, respectively [27].

Potentiodynamic polarization measurements (PDP): Fig. 3 shows Tafel plots of the 316 L SS into 20% HCl solution in absence and the presence of naphthyridine inhibitors (**NP1**, **NP2** and **NP3**) in the range of –250 to +250 mV at the scan rate of 2 mV s^{-1}. The PDP method was used to investigate corrosion efficiency of metal surface from corrosion potential E_{corr} and corrosion current density (I_{corr}). The corrosion kinetic parameters, including the corrosion potential (E_{corr}), corrosion current density (I_{corr}), anodic Tafel slope (β_a) and inhibition efficiency (IE), were determined to evaluate the corrosion behaviour of the system for three inhibitors are presented in Table-4. Fig. 3a shows the I_{corr} values decreased by increase the concentration while inhibition efficiency increases and the highest inhibition efficiency is 74.1% at 40 ppm concentration. Fig. 3b shows the Tafel plots in absence and presence of **NP2** inhibitor. It shows the I_{corr} values decreased by increase the concentration while inhibition efficiency increases and the maximum inhibition efficiency is 81.6% at 40 ppm concentration. Fig. 3c shows the Tafel plots in absence and the presence of **NP3** inhibitor. It shows the I_{corr} values decreased by increase the concentration while inhibition efficiency increases and the maximum inhibition efficiency is 79.8% at 30 ppm concentration. The polarization studies reveal that I_{corr} values are decreased by increasing the concentration of inhibitors, the inhibition efficiency increases. This may be due to the adsorption of the functional groups in inhibitors on the 316 L SS surface and it can be noted that E_{corr} be more than 85 mV, the synthesized inhibitors can act as an anodic or cathodic type, so studied naphthyridine inhibitors (**NP1**, **NP2** and **NP3**) are mixed-type inhibitors. The polarization results finalized that three inhibitors (**NP1**, **NP2** and **NP3**) provide the good corrosion against 316L SS in 20% HCl solution. The **NP2** has the highest corrosion inhibition efficiency of 81.6% at 40 ppm concentration, because of heteroatoms of **NP2** attached more than other two inhibitors on metal surface and follows the order of **NP2** > **NP3** > **NP1** [28].

Weight loss measurements

Effect of inhibitor concentration: The corrosion inhibition of three inhibitors (**NP1**, **NP2** and **NP3**) on 316L SS in

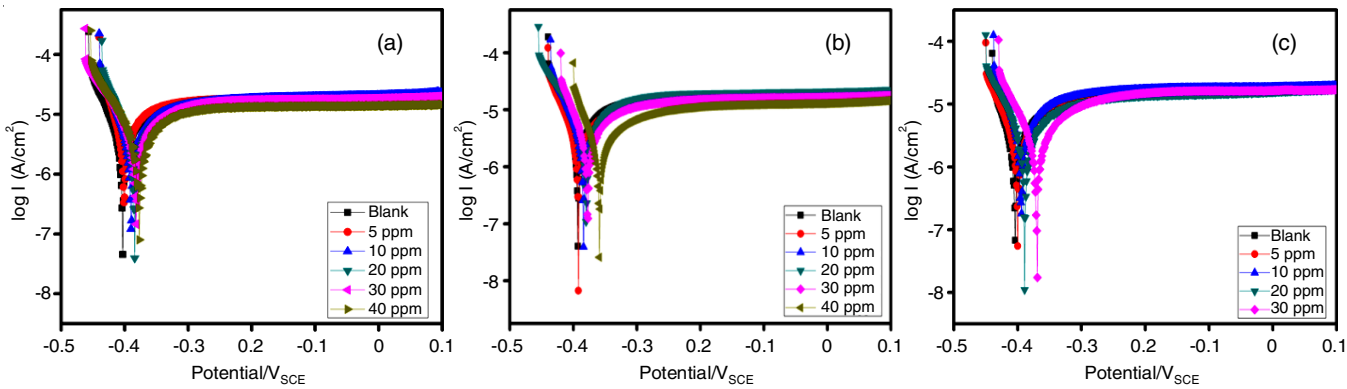

Fig. 3. Tafel plots of (a) **NP1** (b) **NP2** (c) **NP3** on potentiodynamic measurement curves of 316L SS in 20% HCl solution

TABLE-4
PDP PARAMETERS OF 316L SS IN 20% HCl SOLUTION FOR THREE INHIBITORS (**NP1**, **NP2** AND **NP3**)

Inhibitor conc. (ppm)	NP1			NP2			NP3		
	E_{corr} (mV)	I_{corr} (μA)	IE (%)	E_{corr} (mV)	I_{corr} (μA)	IE (%)	E_{corr} (mV)	I_{corr} (μA)	IE (%)
Blank	-403	14.82	–	-393	24.87	–	-404	19.34	–
5	-400	7.862	46.9	-390	11.326	54.4	-399	9.673	49.9
10	-388	6.247	57.8	-383	9.782	60.6	-393	6.139	68.2
20	-384	5.139	65.3	-380	7.146	71.2	-388	5.371	72.2
30	-380	4.263	71.2	-376	5.739	76.9	-368	3.893	79.2
40	-375	3.837	74.1	-358	4.567	81.6	-386	4.592	76.2
50	-378	4.611	68.8	-373	5.368	78.4	-375	5.693	70.5
70	-384	5.249	64.5	-381	6.674	73.1	-371	7.437	61.5
100	-388	5.930	59.9	-389	7.292	70.6	-364	8.103	58.1

20% HCl solution by weight loss method, which involves measuring the change in weight of the material over a specified period to determine the corrosion rate. It was studied by three inhibitors with different immersion times such as 168, 336, 504 and 672 h at room temperature. Table-5 shows the weight loss values, corrosion rate values and inhibition efficiency of naphthyridine inhibitors. From weight loss method, corrosion rate values are decreased by increasing inhibitor concentration, the decreased corrosion rate due to adsorption of naphthyridine inhibitor molecules on metal surface of 316 L SS. The corrosion rate of **NP1** inhibitor decreases due to molecules in **NP1** inhibitor and the inhibition efficiency (IE%) increases by increasing the concentration up to 40 ppm, further no significant changes occurred after increase the concentrations (Table-5). The highest inhibition efficiency of **NP1** inhibitor 72.6% from the weight-loss method, which may be due to the efficient group present in the **NP1** inhibitor. Similarly, corrosion rate of **NP1** inhibitor decrease and inhibition efficiency (IE%) increase by increasing the concentration up to 40 ppm, further no changes after increasing the **NP2** concentrations. The maximum inhibition efficiency of the **NP2** inhibitor is 80.4% from the weight-loss method, which may be due to the chloro group present in **NP2** inhibitor. The corrosion rate of **NP3** inhibitor decrease and inhibition efficiency increase by increasing the concentration upto 30 ppm, no significant changes after 30 ppm concentrations. The maximum inhibition efficiency for **NP3** inhibitor is 77.6%, which may be the functional group especially bromo present in **NP3** inhibitor. The inhibition efficiency for three inhibitors is 72.6% for **NP1**, 80.4% for **NP2** and 77.6% for **NP3** inhibitors. The maximum inhibition efficiency observed for **NP2** inhibitor of 80.4% obtained from the weight-loss method, which may be owing to strong electric character of the functional groups is responsible for the observed phenomena, as these groups play a crucial role in determining the electrostatic interactions and overall molecular properties may be chloro group interrelate more on the surface of 316 L SS present in the **NP2** inhibitor [29].

Effect of immersion time: The effect of different immersion time at 168, 336, 504 and 672 h in presence and the absence of naphthyridine inhibitors (**NP1**, **NP2** and **NP3**) were studied on 316 L SS in 20% HCl solution using the weight loss method. Fig. 4 shows the variation of inhibition efficiency (IE%) *vs.* different immersion times, the IE% of three inhibitors reveal the more inhibition efficiency occurs in more immersion time it forms a protective film over the surface of 316 L SS metal. In Table-5, the weight loss values and the corrosion rate values are decreased by increase the immersion time from 168 to 672 h for **NP1** naphthyridine inhibitor. It can be observed that maximum inhibition efficiency of 72.6% for **NP1** at 40 ppm in 672 h of immersion time. No changes to be observed after 40 ppm. The weight loss value and corrosion rate values are decreased by increase the immersion time from 168 to 672 h for **NP2** inhibitor. It can be noted that utmost inhibition efficiency of 80.4% for **NP2** by 40 ppm in 672 h of immersion time. No changes was observed after 40 ppm for **NP2** inhibitor. Then the weight loss and corrosion rate values are decreased

TABLE-5
WEIGHT LOSS DEPTH STUDY OF 316L SS FOR **NP1**, **NP2** AND **NP3** INHIBITORS

Inhibitors	Conc.	Corrosion rate (mm/year)				IE (%)			
		168 h	336 h	504 h	672 h	168 h	336 h	504 h	672 h
	Blank	9.628	14.814	19.339	24.914	–	–	–	–
	5	8.114	11.479	13.962	16.843	15.7	22.5	27.8	32.3
	10	7.239	9.746	11.355	13.529	24.8	34.2	41.2	45.6
	20	5.968	7.315	8.731	10.362	38	50.6	54.8	58.4
NP1	30	4.325	5.693	7.192	8.517	55	61.5	62.8	65.8
	40	3.565	4.765	5.512	6.813	62.9	67.8	71.4	72.6
	50	4.146	5.937	6.135	7.154	56.9	59.9	68.2	71.2
	70	5.327	6.355	7.986	9.793	44.6	57.1	58.7	60.6
	100	6.762	7.612	8.737	10.406	29.7	48.6	54.8	58.2
	Blank	12.091	14.790	17.537	21.962	–	–	–	–
	5	10.659	12.968	15.012	18.037	11.8	12.3	14.3	17.8
	10	9.271	10.544	12.179	14.892	23.3	28.7	30.5	32.1
	20	7.533	8.813	10.108	12.114	37.6	40.4	42.3	44.8
NP2	30	4.982	5.648	6.392	7.270	58.7	61.8	63.5	66.8
	40	2.971	3.419	3.873	4.284	75.4	76.8	77.9	80.4
	50	3.719	4.103	4.571	5.475	69.2	72.2	73.9	75
	70	5.470	6.592	7.435	8.869	54.7	55.4	57.6	59.6
	100	7.963	9.247	9.247	10.108	34.1	43.4	47.2	53.9
	Blank	9.534	13.617	16.933	20.574	–	–	–	–
	5	8.090	9.753	10.871	11.750	15.1	28.3	35.7	42.8
	10	6.674	7.368	8.926	9.604	29.9	45.8	47.2	53.3
	20	4.592	5.609	6.794	7.399	51.8	58.8	59.8	64
NP3	30	2.937	3.394	3.989	4.593	69.1	75	76.4	77.6
	40	4.678	5.671	6.873	7.891	50.9	58.3	59.4	61.6
	50	6.951	7.093	8.419	9.733	27	47.9	50.2	52.6
	70	7.563	10.245	11.642	12.556	20.6	24.7	31.2	38.9
	100	8.125	11.378	13.732	15.714	14.7	16.4	18.9	23.6

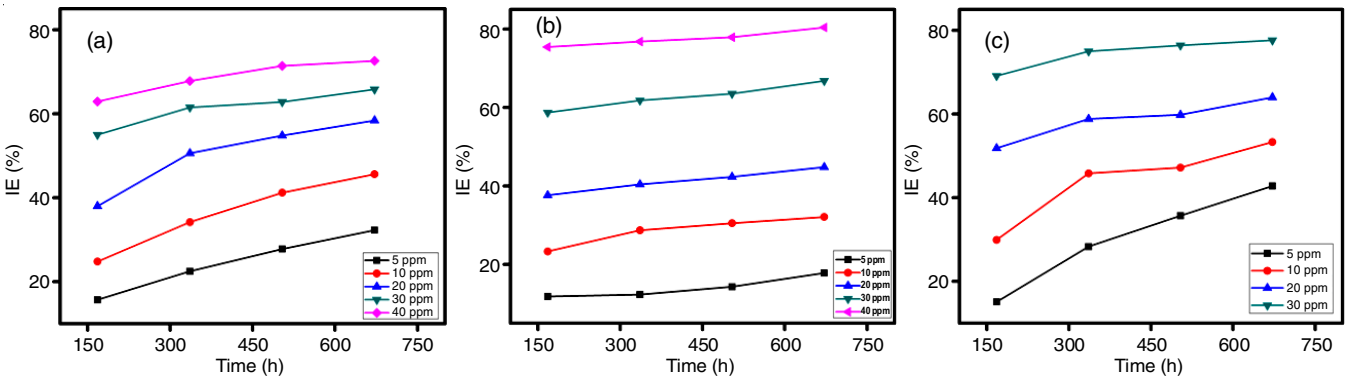

Fig. 4. Plot diagram of IE% against immersion time (a) **NP1** (b) **NP2** and (c) **NP3** inhibitors immersed in 20% HCl solution

by increase the immersion time from 168 to 672 h for **NP3** naphthyridine inhibitor. The maximum inhibition efficiency of **NP3** inhibitor is 77.6% at 30 ppm for 672 h of immersion time. There is no changes occurred after 30 ppm for **NP2** inhibitor. From the results of consequence of immersion time, decrease in the corrosion rate owing to more adsorption of naphthyridine inhibitor molecules on 316 L SS exterior. On comparing the inhibitors, **NP2** shows the highest inhibition efficiency of 80.4% at 40 ppm due to more number of heteroatoms present when compared to other two inhibitors. The order of inhibition efficiency of the various inhibitors is as follows: **NP2** > **NP3** > **NP1**.

SEM studies: The absence and presence of naphthyridine inhibitors on the surface of 316 L SS layer was investigate by Scanning electron microscopy (SEM). Fig. 5 shows the SEM image of metal exterior in the absence and the presence of naphthyridine inhibitors (**NP1**, **NP2** and **NP3**) immersed for 24 h of time. Fig. 5 (blank) shows the cracked surface resulting

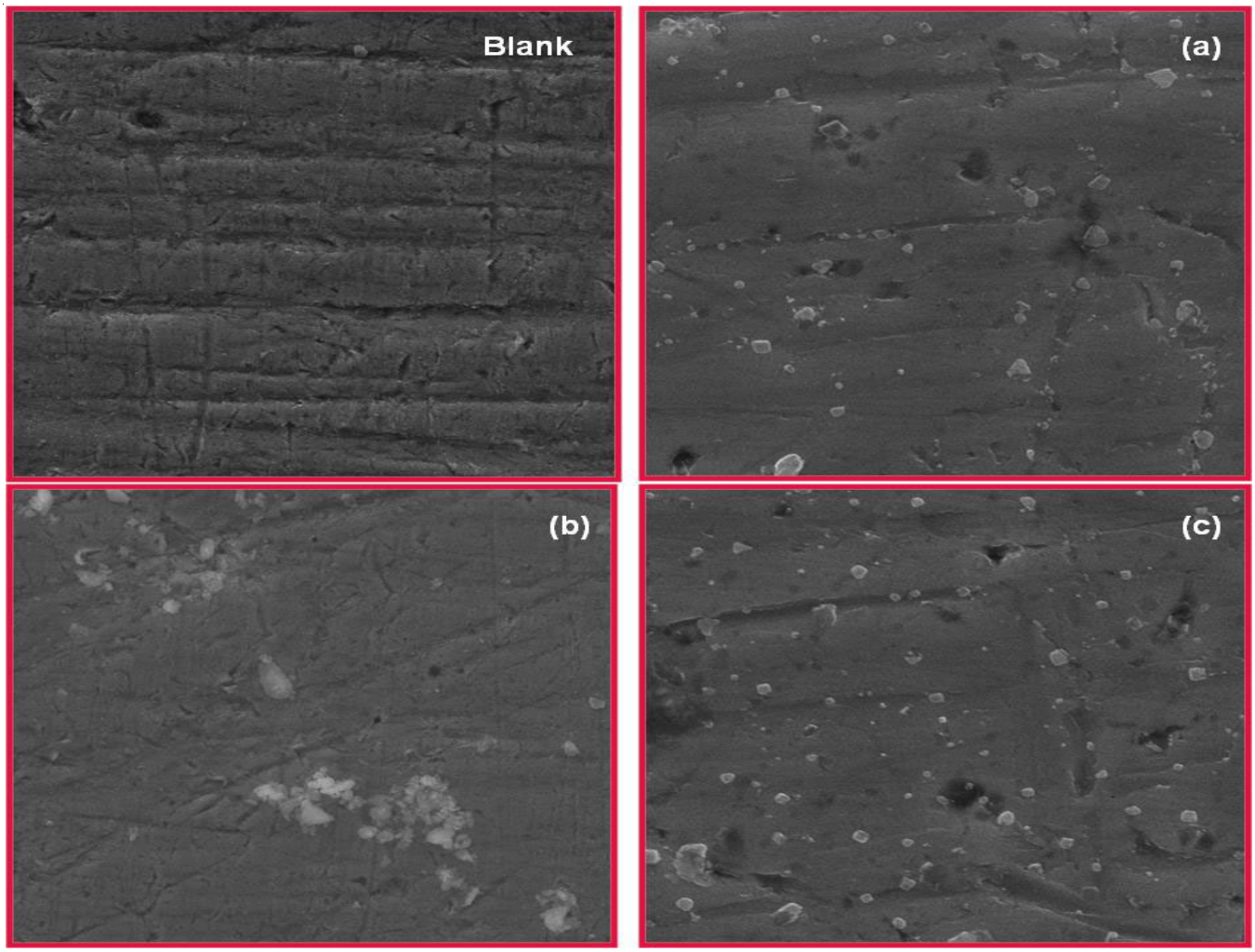

Fig. 5. SEM image of blank, (a) **NP1** (b) **NP2** (c) **NP3** inhibitors immersed in 20% HCl solution for 24 h

from the lack of an inhibitor on the steel surface, as the ions in the environment have minimal impact on the metal surface. Fig. 5a-c indicates that the inhibitor molecules actively adsorbed the metal surface of 316 L SS to form a protective layer, this may due to functional groups present in inhibitors participated the metal surface to decrease the corrosion. Further, the SEM image in presence of inhibitors reveals the metal exterior is smoother and protected [30].

Conclusion

It has been concluded that successful utilization of malononitrile dimer as a precursor for the synthesize of 1,6-naphthyridine derivatives from aromatic aldehyde by one pot synthesis. It was characterized by spectral analysis of ^{1}H NMR, ^{13}C NMR, IR and UV-Vis techniques. Due to their distinctive structure, the significant antimicrobial inhibition against both Gram-positive and Gram-negative bacteria were evaluated. Furthermore, the synthesized three naphthyridine derivatives are quite interesting to explore in corrosion inhibition studies using 316 L SS in 20% HCl solution by electrochemical impedance spectroscopy, potentiodynamic polarization measurement, weight loss method. The EIS shows inhibition efficiency of **NP1** 76.4% at 40 ppm, **NP2** 83.7% at 40 ppm and 82.3% at 30 ppm and **NP2** has the uppermost inhibition efficiency of 83.7% was observed at 30 ppm concentration. The PDP results also indicates the **NP2** has the peak corrosion inhibition efficiency of 81.6% was obtained at 40 ppm concentration and act as mixed type inhibitor. The weight loss study revealed that the inhibition efficiency of 74.1% for **NP1** at 40 ppm, 81.6% for **NP2** at 40 ppm and 79.8% for **NP3** at 30 ppm were observed. The highest inhibition of all the studies due to the functional groups in inhibitors powerfully adsorbed on the exterior of 316 L SS and it forms a protective film to avoid corrosion activities. The SEM analysis indicates that all the inhibitors are strongly adsorbed on surface of the 316L SS in the form of a protective layer. The inhibition efficiencies follow the order of **NP2 > NP3 > NP1** and the greatest inhibition efficiency of 83.7% at 40 ppm concentration for **NP2** inhibitor. Finally, the corrosion result of three inhibitors shows that **NP2** act as more inhibiting properties than other two on 316 L SS in 20% HCl solution.

CONFLICT OF INTEREST

The authors declare that there is no conflict of interests regarding the publication of this article.

REFERENCES

1. A. Madaan, R. Verma, V. Kumar, A.T. Singh, S.K. Jain and M. Jaggi, *Arch. Pharm.*, **348**, 837 (2015); https://doi.org/10.1002/ardp.201500237
2. T. Devadoss, V. Sowmya and R. Bastati, *ChemistrySelect*, **6**, 3610 (2021); https://doi.org/10.1002/slct.202004462
3. S.K. Srivastava, A. Jha, S.K. Agarwal, R. Mukherjee and A.C. Burman, *Anticancer Agents Med. Chem.*, **7**, 685 (2007); https://doi.org/10.2174/187152007784111313
4. V.P. Litvinov, *Adv. Heterocycl. Chem.*, **91**, 189 (2006); https://doi.org/10.1016/S0065-2725(06)91004-6
5. V.V. Dotsenko, S.G. Krivokolysko and A.M. Semenova, *Chem. Heterocycl. Compd.*, **54**, 989 (2018); https://doi.org/10.1007/s10593-018-2383-y
6. M.C. Zerner, C. Reidlinger, W.M.F. Fabian and H. Junek, *J. Mol. Struct. THEOCHEM*, **543**, 129 (2001); https://doi.org/10.1016/S0166-1280(00)00851-4
7. M. Khalid, I. Shafiq, M.A. Asghar, A.A.C. Braga, S.M. Alshehri, M. Haroon and M.L. Sanyang, *Sci. Rep.*, **13**, 20104 (2023); https://doi.org/10.1038/s41598-023-44327-9
8. M.Y. Belikov, S.V. Fedoseev, M.Y. Ievlev and O.V. Ershov, *Synth. Commun.*, **48**, 2850 (2018); https://doi.org/10.1080/00397911.2018.1500426
9. A.J. Fatiadi, *Synthesis*, 165 (1978); https://doi.org/10.1055/s-1978-24703
10. F. Freeman, *Chem. Rev.*, **69**, 591 (1969); https://doi.org/10.1021/cr60261a001
11. A. Shaabani and S.E. Hooshmand, *Mol. Divers.*, **22**, 207 (2018); https://doi.org/10.1007/s11030-017-9807-y
12. A. Albert and W.L.F. Armarego, *J. Chem. Soc.*, 4237 (1963); https://doi.org/10.1039/jr9630004237
13. S.N. Anjirwala and S.K. Patel, *J. Heterocycl. Chem.*, **61**, 1481 (2024); https://doi.org/10.1002/jhet.4871
14. P. Singh, E.E. Ebenso, L.O. Olasunkanmi, I.B. Obot and M.A. Quraishi, *J. Phys. Chem. C*, **120**, 3408 (2016); https://doi.org/10.1021/acs.jpcc.5b11901
15. S.A.S. Mousa, *Int. J. Chem. Stud.*, **5**, 290 (2017).
16. C. Verma, A.A. Sorour, E.E. Ebenso and M.A. Quraishi, *Results Phys.*, **10**, 504 (2018); https://doi.org/10.1016/j.rinp.2018.06.054
17. M. Salman, K.R. Ansari, V. Srivastava, D.S. Chauhan, J. Haque and M.A. Quraishi, *J. Mol. Liq.*, **322**, 114825 (2021); https://doi.org/10.1016/j.molliq.2020.114825
18. R. Ansari and F. Sadeghi, *Physica E*, **69**, 1 (2015); https://doi.org/10.1016/j.physe.2015.01.009
19. F. Wedian, I. Mhaidat, N.A. Braik and G.M. Al-Mazaideh, *Int. J. Corros. Scale Inhib.*, **11**, 364 (2022); https://doi.org/10.17675/2305-6894-2022-11-1-22
20. G. Vengatesh and M. Sundaravadivelu, *J. Adhes. Sci. Technol.*, **34**, 2075 (2020); https://doi.org/10.1080/01694243.2020.1750808
21. R.A. Carboni, D.D. Coffman and E.G. Howard, *J. Am. Chem. Soc.*, **80**, 2838 (1958); https://doi.org/10.1021/ja01544a061
22. M. Packiaraj and K.K.S. Kumar, *J. Alloys Compd.*, **864**, 158345 (2021); https://doi.org/10.1016/j.jallcom.2020.158345
23. A.O. Yüce and G. Kardas, *Corros. Sci.*, **58**, 86 (2012); https://doi.org/10.1016/j.corsci.2012.01.013
24. M.A. Amin, S.S. Abd El-Rehim, E.E.F. El-Sherbini and R.S. Bayoumi, *Electrochim. Acta*, **52**, 3588 (2007); https://doi.org/10.1016/j.electacta.2006.10.019
25. I.N. Bardasov, A.U. Alekseeva, V.A. Tafeenko and O.V. Ershov, *Synth. Commun.*, **49**, 3343 (2019); https://doi.org/10.1080/00397911.2019.1665184
26. M. Badawneh, L. Bellini, T. Cavallini, J.A. jamal, C. Manera, G. Saccomanni and P.L. Ferrarini, *Farmaco*, **58**, 859 (2003); https://doi.org/10.1016/S0014-827X(03)00144-7
27. X. Li, S. Deng and H. Fu, *Corros. Sci.*, **62**, 163 (2012); https://doi.org/10.1016/j.corsci.2012.05.008
28. R.H. Tammam, A.S. Mogoda and M.H. Gharbawy, *Int. J. Electrochem. Sci.*, **15**, 8408 (2020); https://doi.org/10.20964/2020.09.13
29. M.A. Deyab and S.S.A. El-Rehim, *Int. J. Electrochem. Sci.*, **8**, 12613 (2013); https://doi.org/10.1016/S1452-3981(23)13293-7
30. A. Seikh, A. Mohammad, E.-S. Sherif and A. Al-Ahmari, *Metals*, **5**, 2289 (2015); https://doi.org/10.3390/met5042289